

ON THE ORIGIN OF SUPERNOVA-LESS LONG GAMMA RAY BURSTS

SHLOMO DADO¹ AND ARNON DAR¹

¹*Physics Department, Technion, Haifa 32000, Israel*

ABSTRACT

The fraction of long duration gamma ray bursts (GRBs) without an associated bright supernovae (SNe) at small redshifts ($z < 0.15$) is comparable to that of GRBs associated with SNe. We show, that their X-ray afterglow and those of most of the nearby ($z < 1$) GRBs without a confirmed association with SNe, are well reproduced by the launch of highly relativistic jets in the SN-less birth of millisecond pulsars (MSPs) in neutron star mergers or through phase transition of neutron stars to quark stars following mass accretion in compact binaries. Such a large fraction of GRBs with pulsar-like afterglow that extends to very large redshifts ($z > 4$) favors phase transition of neutron stars to quark stars in high mass X-ray binaries (HMXBs) rather than neutron stars mergers as their origin.

Keywords: gamma-ray burst, jets, neutron star

1. INTRODUCTION

Gamma ray bursts seem to be divided into two distinct classes, long duration soft gamma ray bursts (GRBs) that usually last more than 2 seconds and short hard bursts (SHBs) that usually last less than 2 seconds (Norris et al. 1984; Kouveliotou et al. 1993). While there is clear photometric (e.g., Dado et al. 2002, Zeh et al. 2004) and spectroscopic evidence (e.g., Della Valle et al. 2016 and references therein) that a large fraction of the long duration GRBs are produced in very bright stripped envelope supernova (SN) explosions of type Ic (Galama et al. 1998), there is also evidence that supernova explosions are not the only source of long duration GRBs (e.g., Della Valle et al. 2006; Fynbo et al. 2006; Gal-Yam et al. 2006). Moreover, in the local universe the rate of SN-less GRBs is comparable to that of SN-GRBs, as can be seen from Table 1 where all the GRBs with known redshift $z < 0.15$ are listed. If that is valid universally, then the fraction of SN-less GRBs is comparable to that of SN-GRBs. The origin of such a large population of SN-less GRBs, which seems to extend to very large redshifts is still unknown.

Thirty years ago, Goodman, Dar and Nussinov (1987) suggested that GRBs are not Galactic in origin, as was widely believed, but may be produced at cosmological distances by highly relativistic $e^+e^-\gamma$ fireballs (Goodman 1986) formed by neutrino-antineutrino annihilation around merging neutron stars in close binaries due to gravitational wave emission and/or around compact stars undergoing gravitational collapse due to mass accretion. But, shortly after the launch of the Compton gamma ray burst observatory (CGRO), it became clear that such neutrino-annihilation fireballs are not powerful enough to produce observable GRBs at the very large cosmological distances, which were indicated by the CGRO observations (Meegan et al. 1992). Consequently, Meszaros and Rees (1992) suggested that the $e^+e^-\gamma$ fireballs produced in the merger of neutron stars and of neutron stars and stellar black holes may be collimated into $e^+e^-\gamma$ jets by funneling through surrounding matter. Instead, Shaviv and Dar (1995) suggested that GRBs are produced at large cosmological distances by inverse Compton scattering (ICS) of ambient light by narrowly collimated jets of plasmoids (cannonballs) of ordinary matter rather than by collimated fireballs, launched in neutron star mergers, in phase transition of neutron stars to quark stars in compact binaries due to mass accretion, and in stripped envelope SN explosions. To date, there is direct photometric and spectroscopic evidence for production of GRBs in stripped envelope SNe of type Ic (see, e.g., Della Valle 2016 and references therein), but only indications that SHBs and perhaps

SN-less GRBs may be produced in neutron star mergers (Tanvir et al. 2013; Berger et al. 2013; Hotokezaka et al. 2013; Fong and Berger 2014, Berger 2014, and Jin et al. 2015, respectively).

There is, however, compelling evidence that both GRBs and SHBs are produced by inverse Compton scattering (ICS) of light by highly relativistic jets (Shaviv & Dar 1995). It includes a large linear polarization of the prompt emission, pulse shape and spectral evolution during its fast decline phase, and various correlations among burst properties (see, e.g., Dar & De Rújula 2000, 2004; Dado et al. 2009a,b; Dado & Dar 2017 and references therein). The main suggested sources of such highly relativistic jets, other than SN explosions, include merger of neutron stars (Goodman, Dar & Nussinov 1987), neutron star - black hole mergers (Meszaros & Rees 1992), phase transition of neutron stars to more compact objects (quark stars or black holes) following mass accretion from a companion star (Dar et al. 1992), and "failed supernovae" (FSN), i.e., direct collapse of massive stars to black holes without a supernova (e.g., Woosley 1993a,b). These different types of events are likely to produce different afterglows and different gravitational wave signals, which may be used to identify the origin of SN-less GRBs.

An FSN origin of SN-less GRBs seems to be ruled out: Both FSN-GRBs and SN-GRBs are produced by highly relativistic jets emitted in core collapse of massive stars which takes place mostly within dense molecular clouds. In such environments, their late-time afterglows are dominated by synchrotron radiation emitted by the decelerating jets in their high density circumburst environment. Such synchrotron afterglows satisfy simple closure relations between their late-time spectral and temporal behaviors (e.g., Dar & De Rújula 2004; Dado & Dar 2013,2017) independent of the jet origin. However, the observed late-time afterglows of SN-less GRBs that are expected to be powered by millisecond pulsars (MSPs) are different from those of SN-GRBs (e.g., Cano et al. 2017) and do not satisfy the standard closure relations of SN-GRBs afterglows.

Among the other alternative sources of SN-less GRBs, either merger or phase transition of neutron stars within globular clusters (GCs) of very high density interstellar light and very low density interstellar medium (ISM) may explain the observed late-time X-ray afterglow of SN-less GRBs. Indeed, in this paper we show that the light curves of the X-ray afterglow of the well sampled nearby SN-less GRBs measured with the Swift X-ray telescope (Evans et al. 2007, 2009) are well explained by ICS of GC light by relativistic jets launched in the birth of an MSP, which is taken over by an X-ray af-

terglow powered by the spin down of the newly born MSP (Dai and Lu 1998a,b; Zhang and Meszaros 2001; Dai et al. 2006; Metzger et al. 2008). Late time afterglows powered by MSPs rule out neutron star - black hole mergers or phase transition of neutron stars to black holes as the origin of SN-less GRBs. However, they do not distinguish between neutron stars merger origin and collapse of neutron stars to quark stars following mass accretion. But, in this paper, we also show that the fraction of GRBs with a very large measured redshift ($z > 4$), which have "MSP-like" late-time X-ray afterglow (12 out of 24), is like that observed at very low redshifts ($z < 0.15$). It implies the same redshift dependence of the production rate of SN-less GRBs and SN-GRBs. It favors mass accretion on neutron stars in high mass (short lived) X-ray binaries (HMXBs) as the origin of SN-less GRBs (Dar 1998) rather than merger of neutron stars in compact binaries by gravitational wave emission which takes time comparable to the age of the universe.

2. THE FAST DECLINE PHASE OF PROMPT EMISSION

Consider first a jet which is a succession of highly relativistic plasmoids (cannonballs) launched during the birth of MSP in neutron star merger or phase transition in a close binary within a collapsed core of a globular cluster. Let γ be the bulk motion Lorentz factor of such a cannonball (CB) and $\delta = 1/(1 - \beta \cos\theta)$ be its Doppler factor when viewed at an angle θ relative to its direction of motion. As long as the CB moves inside the collapsed core, ICS of its nearly isotropic light by the plasmoid electrons produces a light curve proportional to the light density along its trajectory. As the highly relativistic CB leaves the collapsed core and moves away, the angle between the CB motion and the intercepted GC photons decreases with distance r from the GC core like r/R_c , where R_c is the radius of the collapsed core of the GC. The transverse momentum of the intercepted GC photons in the CB rest frame is unchanged, while their parallel component is strongly red shifted. Hence, in the plasmoid rest frame, the energy ϵ of an intercepted GC photon is Lorentz transformed to an energy $(R_c/r)\epsilon$. This energy is Doppler boosted by ICS to an energy $E \approx R\epsilon/(1+z)r$ when observed at a viewing angle θ in the rest frame of a distant observer. Time aberration yields a distance $r = c\gamma\delta t/(1+z)$ of the CB from the GC at an observer time t . Hence, for a GC light with a bremsstrahlung-like spectrum, $\epsilon^2 dn/d\epsilon \propto \exp(-\epsilon/\epsilon_p)$ and a density $n \propto 1/r^2$ at $r \gg R_c$, the decay of the energy density flux $F(t)$ from ICS of a GC light by a highly relativistic plasmoid launched at $t = 0$ is given

by (Dado and Dar 2017),

$$F(t) = E^2 dN/dE \propto \exp(-t/\tau) \quad (1)$$

with $\tau(E) \approx 100(R_c/pc)(\epsilon_p/eV)/c(E/keV)(\gamma/10^3)$ s. This decay rate of the prompt emission depends strongly on the observed energy band. It is valid only when $r \gg R_c$, i.e., for $t \gg t_{es}$, where t_{es} is the escape time of the highly relativistic plasmoids from the GC core at redshift z , as observed by a distant observer from a viewing angle $\theta \approx 1/\gamma$. The E -dependence of τ produces the observed (Evans et al. 2007, 2009) fast spectral softening as function of time during the exponential decline of the prompt emission for $t > t_{es}$. Due to time aberration, $t_{es} \approx (1+z)R_c/\gamma\delta c$. The median value of the observed radii of collapsed cores of GCs is $R_c \sim 1$ pc. Hence, $t_{es} \approx (1+z)50$ s, for a plasmoid with $\delta \approx \gamma \approx 500$, which is similar to the typical time that the Swift-XRT usually begins its follow-up observations.

The successive emission of plasmoids during a GRB and/or a bumpy light density in the globular cluster yields a bumpy light curve, with resolved peaks at early times because of large photon statistics. Later, when the luminosity decreases, the larger time bins (and perhaps merger of CBs) yield smoothly appearing light curves. The smoothed X-ray light-curve during the fast decay phase of the prompt ICS emission from the jet is expected to be described roughly by

$$F_j(t) \approx \frac{a F_j(0)}{a + (t/\tau)\exp(t/\tau)} \quad (2)$$

where a is an adjustable parameter. The radius of large GCs can reach $R \approx 25$ pc. If the GRB occurred within the collapsed core (cc) of a large GC, ICS of the quasi isotropic GC light by the CB inside the GC can take over during the fast decay of the contribution from the collapsed core, and produce a second bump with a shape given also by Eq.(2), but with a much smaller $F_j(0)$, $\tau_{GC} \gg \tau_{cc}$, and $t_{es} \approx (1+z) \times 10^4 (R/25 pc)(\gamma/500)^2$, which is taken over during its fast decay phase by the MSP contribution.

The light-curve of a late GRB pulse, or a flare during the decline of the prompt emission, which is produced by ICS of ambient light by a CB launched at a time $t_{i,0}$, is given by (e.g., Dar and De Rjula 2004)

$$F_i(t_i) \approx F_i\Delta \frac{4(t_i/\Delta_i)^2}{((t_i/\Delta_i)^2 + 1)^2} \quad (3)$$

where $t_i = t - t_{i,0}$, is the time after $t_{i,0}$ the beginning time of pulse i whose peak value is at $t_i = \Delta_i$. A smooth interpolation from this early time behavior to the late time behavior given by Eq.(1), is provided by

$$F_i(t) = F_{p,i} \frac{2.528(t_i/\Delta_i)^2 \exp(-t_i/\tau_i)}{((t_i/\Delta_i)^2 + 1)^2 (1 - \exp(-\Delta_i/t_i))} \quad (4)$$

where $2.528 = 4(1 - e^{-1})$.

3. AFTERGLOWS POWERED BY MSPS

Newly born neutron stars seem to be surrounded by nearby plerions, which absorb their emitted radiation, winds, and highly relativistic particles, and convert them to luminous energy, mostly in the X-ray band. If the power source is the spin down of a newly born neutron star with a period P , then, in a steady state it generates a plerion luminosity $L(t) = 2\pi^2 I \dot{P}/P^3$. For canonical neutron stars of a radius $R = 10^6$ cm and a mass $M \approx M_{Ch}$, where $M_{Ch} \approx 1.4M_\odot$ is the Chandrasekhar mass limit of white dwarfs, $I = (2/5)M_{Ch}R^2 \approx 1.12 \times 10^{45} g cm^2$.

Observations of young X-ray pulsars indicate that the change of their period during their spin down satisfies to a good approximation,

$$P\dot{P} = K \quad (5)$$

where K is time independent constant (with time-dimension). Such a behavior is expected from pulsars which spin down by magnetic dipole radiation (MDP) from a magnetic dipole aligned at an angle $\alpha > 0$ relative to the rotation axis, and stays constant in time (in the pulsar rest frame) during spin down (e.g., Manchester & Taylor 1977). Observations, however, indicate that $P\dot{P}$ remains constant to a good approximation also when other spin down mechanisms, such as emission of winds and/or highly relativistic particles, contribute, or even dominate the spin-down of pulsars. This follows from the fact that the age estimate $t = [P^2(t) - P^2(0)]/2K$ and the braking relation $d^2P/dt^2 \approx -K^2/P^3$ (Manchester & Taylor, 1977) seem to be satisfied also by young X-ray pulsars: The age relation has been tested by comparing the age obtained from measurements of P and \dot{P} of young pulsars to the known ages of their parent supernovae (historical supernovae) or to their ages obtained from measurements of the distance and proper motion of the young pulsars relative to the centers of the supernova remnants where they were born. The braking relation, which is very difficult to test over a human time scale, has been verified only in few young X-ray pulsars where it yielded a braking index near the expected value 3 (see, e.g., Archibald et al. 2016 and references therein).

We shall assume that Eq.(5) is valid approximately for the power supply by the newly born millisecond neutron stars in SN-less GRBs during the first few days after their birth. It then follows from Eq. (5) that,

$$L_{ps}(t) = L_{ps}(0) (1 + t/t_b)^{-2} \quad (6)$$

with $t_b = P_0/2\dot{P}_0$ and $P_0 = P(t=0)$. The afterglow of a GRB at redshift z that is powered by such a luminos-

ity has a local energy flux density $F(t) = L(t)/4\pi D_L^2$, where D_L is the luminosity distance of the GRB at redshift z , i.e.,

$$F_{ps}(t) = F_{ps}(0) (1 + t/t_b)^{-2}. \quad (7)$$

If only a fraction η of the rotational energy is converted to X-rays, then

$$P_0 = \frac{1}{D_L} \sqrt{\frac{(1+z)\pi\eta_x I}{2F_{ps,x}(0)t_b}}, \quad (8)$$

and its time derivative is $\dot{P}_0 = P_0/2t_b$.

Under the assumptions that the spin down of the newly born neutron star is dominated by radiation from a magnetic dipole \mathbf{m} , which is constant in time and is aligned at a fixed angle α relative to its rotation axis, the peak surface value of the dipole magnetic field $B_p = 2m/R^3$ is at the magnetic poles and it satisfies (Manchester & Taylor 1977)

$$B_p \sin\alpha \approx 6.8 \times 10^{19} [P\dot{P}/s]^{1/2} \text{ gauss}. \quad (9)$$

However, the wide use of Eq.(9) for estimating B_p , cannot be trusted because it assumes that there is no magnetic field decay, that the spin down is in a perfect vacuum, that there are no other spin down mechanisms in operation, such as emission of a wind, relativistic particles, and gravitational waves, and that other sources such as thermal energy, stress energy, phase transition and gravitational contraction can be ignored.

4. COMPARISON WITH OBSERVATIONS

Eq. (2) and (7) can be combined to yield the canonical light curve of the decay of the prompt emission phase of SN-less GRBs taken over by a MSP powered afterglow,

$$F(t) \approx \frac{a F(0)}{a + (t/\tau) \exp(t/\tau)} + \frac{F_{ps}}{(1 + t/t_b)^2}. \quad (10)$$

Figures 1-4, show the X-ray light curves of the four nearest SN-less GRBs, 051109B, 080517, 060614, and 050826, with known redshifts and a well-sampled X-ray afterglows, which were measured with the Swift-XRT and are reported in the Swift-XRT GRB light curve repository (Evans et al. 2007,2009). Also shown are their best fit light curves as give by Eq.(10) with the minimal number of parameters. The best fit values of these parameters (2 for the late-time MSP contribution and 2 or 3 for the jet contribution) are listed in Table 2.

We have also verified that all other well sampled X-ray afterglows of GRBs with redshift $z < 1$, which were reported in the Swift-XRT and have no evidence for an associated SN, despite their relative proximity, could be

well fit by Eq.(10) (18 additional GRBs in Figures 5-7), or by Eq.(4) plus Eq.(7) (6 additional GRBs in Figure 8) with flaring activity during the decay phase of their prompt emission.

Moreover, Figures 9 and 10 show the well-sampled X-ray afterglows of 12 GRBs out of 24 with a known large redshift ($z > 4$) that were reported in the Swift-XRT GRB light curve repository (Evans et al. 2007,2009) and could be well fit by a jet + MSP light curve with the parameters listed in Table 4 as shown in these figures.

5. DISCUSSION

Fast rotating millisecond neutron stars can be produced in SN explosions, in merger of neutron stars and by spin up of neutron stars by mass accretion in compact binaries. We have conjectured that the spin down of such newly born young millisecond neutron stars satisfy to a good approximation, $P\dot{P} = K$ where K is constant in time during the first few days after birth. This conjecture was motivated by the fact that the braking relation $d^2P/dt^2 \approx -\dot{P}^2/P \approx -K^2/P^3$ and the age estimate $t_{age} \approx P/2\dot{P}$, which follow from the relation $P\dot{P} \approx const$ seem to be satisfied to a good approximation by young X-ray MSPs: Their braking index derived from precise measurements of $P(t)$ of a few young MSPs is near 3, and the age relation $t_{age} = (P^2 - P_0^2)/2P\dot{P}$ of young pulsars seem to agree with the age of their parent historical supernovae or their age extracted from their observed distance and proper motion relative to the centers of their parent supernovae.

We have shown that all the well sampled light curves of the X-ray afterglow of the nearby SN-less GRBs measured with the Swift X-ray telescope are those expected from the launch of highly relativistic jets in the birth of MSPs within an environment of a very dense light and a very low ISM density. Such an environment exists in stellar-rich GCs within or without a collapsed core. We have also shown that roughly half of all GRBs with well sampled X-ray afterglow, where SN-GRB association has not or could not be confirmed, could be well explained by ICS of light by relativistic jets launched in the birth of an MSP within a GC like environment.

The late time behavior of the light curves of the afterglows of SN-less GRBs is very different from that of SN-GRBs. In SN-GRBs, the light curves are well explained by synchrotron radiation from the deceleration of highly relativistic jets in dense molecular clouds within spiral galaxies, where most massive star formation and core

collapse supernovae of type Ic take place. The late-time light curves of SN-less GRBs can neither be explained well by synchrotron radiation from the deceleration of highly relativistic jets nor do they satisfy the closure relations which are satisfied by the late time afterglows of SN-GRBs.

The MSP birth periods obtained from our fits to the late time X-ray afterglow of SN-less GRBs with known redshift are all well above the minimal classical period $2\pi R/c \approx 0.2$ ms of fast rotating canonical neutron stars.

Late-time afterglows powered by MSPs rule out neutron star - black hole mergers or phase transition of neutron stars to black holes as the origin of SN-less GRBs. However, they do not distinguish between neutron stars merger origin or collapse of neutron stars to quark stars following mass accretion.

SHBs are observed near/within both spiral and elliptical galaxies (probably within the collapsed core of stellar rich GCs), while long soft GRBs seems to take place only in spiral galaxies mainly within star formation regions. This suggest that SHBs and SN-less GRBs have different origins: We have found that the fraction of GRBs with very large measured redshifts ($z > 4$), which have "MSP-like" late-time X-ray afterglow is not different from that observed at very low redshifts ($z < 0.15$). This implies a similar redshift dependence of the rate of SN-less GRBs and SN-GRBs, is proportional to the global star formation rate when beaming and threshold effects are taken into consideration (Dado & Dar 2013). Neutron star merger via gravitational wave emission in compact binaries, usually takes a very long time comparable to the age of the universe. If SN-less GRBs were formed by neutron stars merger in compact binaries due to gravitational wave emission, it would have implied a much lower fraction of SN-less GRBs at very large redshifts, i.e., a much smaller fraction of GRBs which have a late-time X-ray afterglow that appears to be powered by MSP. That is not observed. We have found that out of the 30 GRBs with a measured redshift $z > 4$ about half have a late time X-ray afterglows similar to those of the SN-less GRBs at low- z ($z < 0.15$), which consist about half of the low z GRBs. This favors phase transition of neutron stars to quark stars due to mass accretion in HMXBs as the origin of SN-less GRBs over merger of neutron stars due to gravitational wave emission in compact binaries. Such HMXBs may be present mostly in GCs and star formation regions in spiral galaxies where winds and SN ejecta have already swept away the initial high density ISM.

REFERENCES

- Archibald, R. F., Gotthelf, E. V., Ferdman, R. D., et al., 2016, ApJ, 819L, 16 [arXiv:1603.00305]
- Berger, E., Fong, W., Chornock, R., 2013, ApJL, 744, L23 [arXiv:1306.3960]

Table 1. The SN-GRBs and SN-less GRBs with known redshift $z \leq 0.15$.

SN	SN-GRB	z	SN-less GRB	Ref.
1998bw	980425	0.0085		Galama et al. 1998
		0.013	111005A	Michalowski et al. 2016
2006ag	060218	0.0331		Pian et al. 2006
2010bh	100316D	0.059		Starling et al. 2011
		0.080 ?	051109B	Perley et al. 2006
		0.0809	060505	Fynbo et al. 2006
		0.0890	080517	Stanway et al. 2015
		0.125	060614	Fynbo et al. 2006
2013dx	130702A	0.145		D’Elia et al. 2015
2016jca	161219B	0.1475		Cano et al. 2017

- Berger, E., 2014 ARA&A, 52, 43 [arXiv:1311.2603]
Cano, Z., Johansson, A. K. G., Maeda, K., 2016, MNRAS, 457, 2761 [arXiv:1601.02610]
Cano, Z., Izzo, L., de Ugarte Postigo, A., et al., 2017 [arXiv:1704.05401]
Dado, S., Dar, A., De Rujula, A., 2002, A&A, 388, 1079 [arXiv:astro-ph/0107367]
Dado, S. & Dar, A., 2013, A&A, 558, A115 (2013) [arXiv:1303.2872]
Dado, S. & Dar, A., 2014, ApJ, 785, 70 [arXiv:1307.5556]
Dado, S. & Dar, A., 2016, PhRvD, 94, 063007 [arXiv:1603.06537]
Dado, S. & Dar, A., 2017, arXiv:1708.04603
Dado, S., Dar, A., De Rujula, A., 2009a, ApJ, 696, 994 [arXiv:0809.4776]
Dado, S., Dar, A., De Rujula, A., 2009b, ApJ, 693, 311 [arXiv:0807.1962]
Dai, Z. G., & Lu, T., 1998a, PRL, 81, 4301 [arXiv:astro-ph/9810332]
Dai, Z. G., & Lu, T., 1998b, A&A, 333, L87 [arXiv:astro-ph/9810402]
Dai, Z. G., Wang, X. Y., Wu, X. F., Zhang, B., 2006, Sci, 311, 1127 [arXiv:astro-ph/0602525]
Dar, A., 1998, [arXiv:astro-ph/9809163]
Dar, A. & De Rujula, A., 2000 [arXiv:astro-ph/0012227]
Dar, A. & De Rujula, A., 2004, PhR, 405, 203 [arXiv:astro-ph/0308248]
Dar, A., Kozlovsky, Ben Z., Nussinov, S., Ramaty, R., 1992, ApJ, 388, 164
D’Elia, V., Pian, E., Melandri, A., et al., 2015, A&A, 577, 116 [arXiv:1502.04883]
Della Valle, M., Chincarini, G., Panagia, N., et al. 2006, Nature, 444, 1050 [arXiv:astro-ph/0608322]
Della Valle, M., AApTr, 2016, 29, Issue 2, 99
Evans, P. A., Beardmore, A. P., Page, K. L., et al., 2007, A&A, 469, 379 [arXiv:0704.0128]
Evans, P. A., Beardmore, A. P., Page, K. L., et al., 2009 MNRAS, 397, 1177 [arXiv:0812.3662]
Fong, W. & Berger, E., 2013, ApJ, 776, 18 [arXiv:1307.0819]
Fynbo, J. P. U., Watson, D., Thone, C., et al. 2006, Nature, 444, 1047
Galama, T. J., Vreeswijk, P. M., van Paradijs, J., et al., 1998, Nature 395, 670 [arXiv:astro-ph/9806175]
Gal-Yam, A., Fox, D., Price, P., et al. 2006, Nature, 444, 1053 [arXiv:astro-ph/0608257]
Goodman, J., 1986, ApJ, 308, L47
Goodman, J., Dar, A., Nussinov, S. 1987, ApJ, 314, L7 (1987)
Hotokezaka, K., Kyutoku, K., Tanaka, M., et al. 2013, ApJL, 778, L16 [arXiv:1310.1623]
Jin, Z., Li, X., Cano, Z., et al. 2015, ApJ, 811, L22 [arXiv:1507.07206]
Kouveliotou, C., et al. 1993, ApJ, 413, L101
Manchester, R. N., & Taylor, J. H. 1977, Pulsars
Meegan, C. A., Fishman, G. J., Wilson, R. B., et al. 1992, Nature, 355, 143
Meszaros, P. & Rees, M. J., 1992, MNRAS, 257, 29
Michalowski, M. J., Xu, D., Stevens, J., et al., 2016 [arXiv:1610.06928]
Metzger, B. D., Quataert, E., Thompson, T. A., 2008, MNRAS, 385, 1455 [arXiv:0712.1233].
Norris, J. P., Cline, T. L., Desai, U. D., Teegarden, B. J., 1984, Nature, 308, 434
Perley, D. A., Foley, R. J., Bloom, J. S., Butler, N. R., 2006, GCN 5387
Pian, E., Mazzali, P. A., Masetti, N., et al. 2006, Nature, 442, 1011 [arXiv:astro-ph/0603530]
Shaviv, N. & Dar, A., 1995, ApJ, 447, 863 [arXiv:astro-ph/9407039]
Stanway, E. R., Levan, A. J., Tanvir, N., et al., 2015, MNRAS, 446, 3911 [arXiv:1409.5791]
Starling, R. L. C., Wiersema, K., Levan, A. J., et al., 2011, MNRAS 411, 2792 [arXiv:1004.2919]
Tanvir, N. R., Levan, A. J., Fruchter, A. S., et al. 2013, Nature, 500, 547 [arXiv:1306.4971]
Troja, E., Cusumano, G., LaParola, V., Mangano, V., Mineo, T., 2006, Nuovo Cim. B121, 1599 [arXiv:astro-ph/0701855]
Woosley, S. E., 1993a, A&AS, 97, 205
Woosley, S. E., 1993b, ApJ, 405, 273
Zeh, A., Klose, S., Hartmann, D. H., 2004, ApJ, 609, 952 [arXiv:astro-ph/0311610]
Zhang, B. & Meszaros, P., 2001, ApJ, 552, L35 [arXiv:astro-ph/0011133]

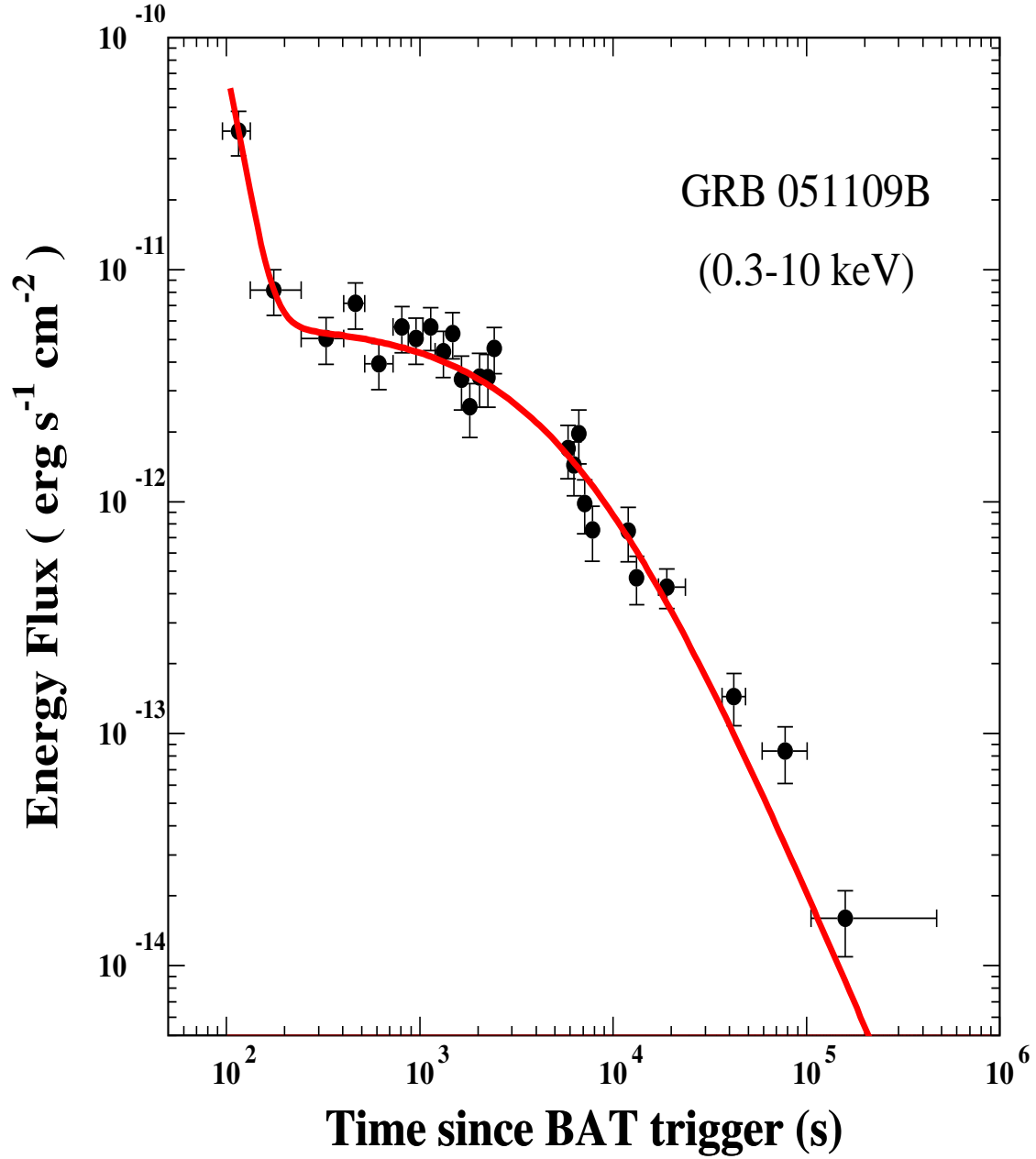


Figure 1. The X-ray light curve of the SN-less GRB 051109B at the (uncertain) redshift $z \approx 0.08$ measured with Swift BAT and XRT telescopes and reported by Troja et al. (2006) and in the Swift-XRT GRB light curve repository (Evans et al. 2007,2009). The line is the best fit light curve as given by Eq.(10) with the parameters listed in Table 2.

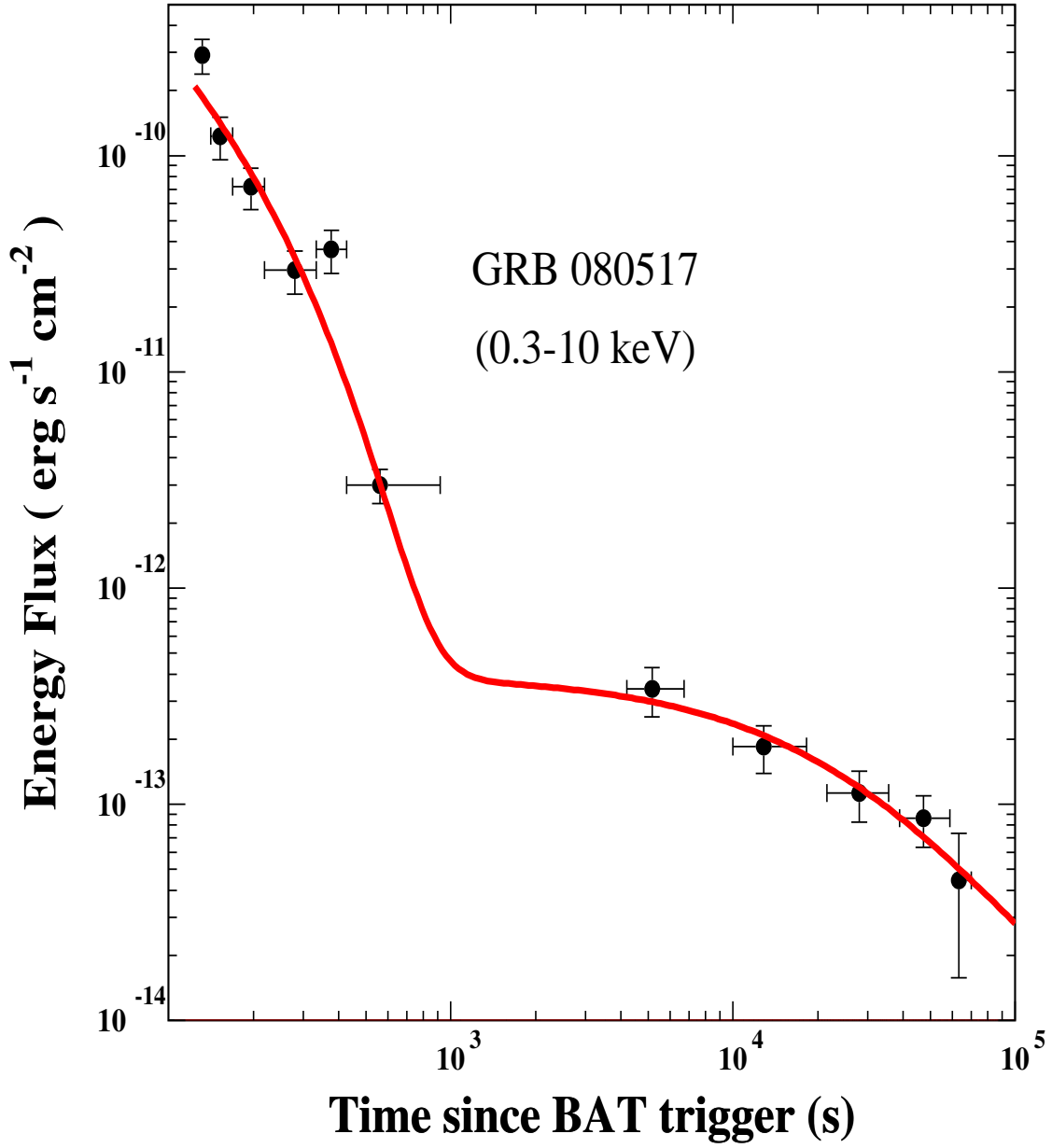


Figure 2. The X-ray light curve of the SN-less GRB080517 at redshift $z = 0.0809$ reported in the Swift-XRT GRB light curve repository (Evans et al. 2007,2009). The line is the best fit light curve as given by Eq.(10) with the parameters listed in Table 2.

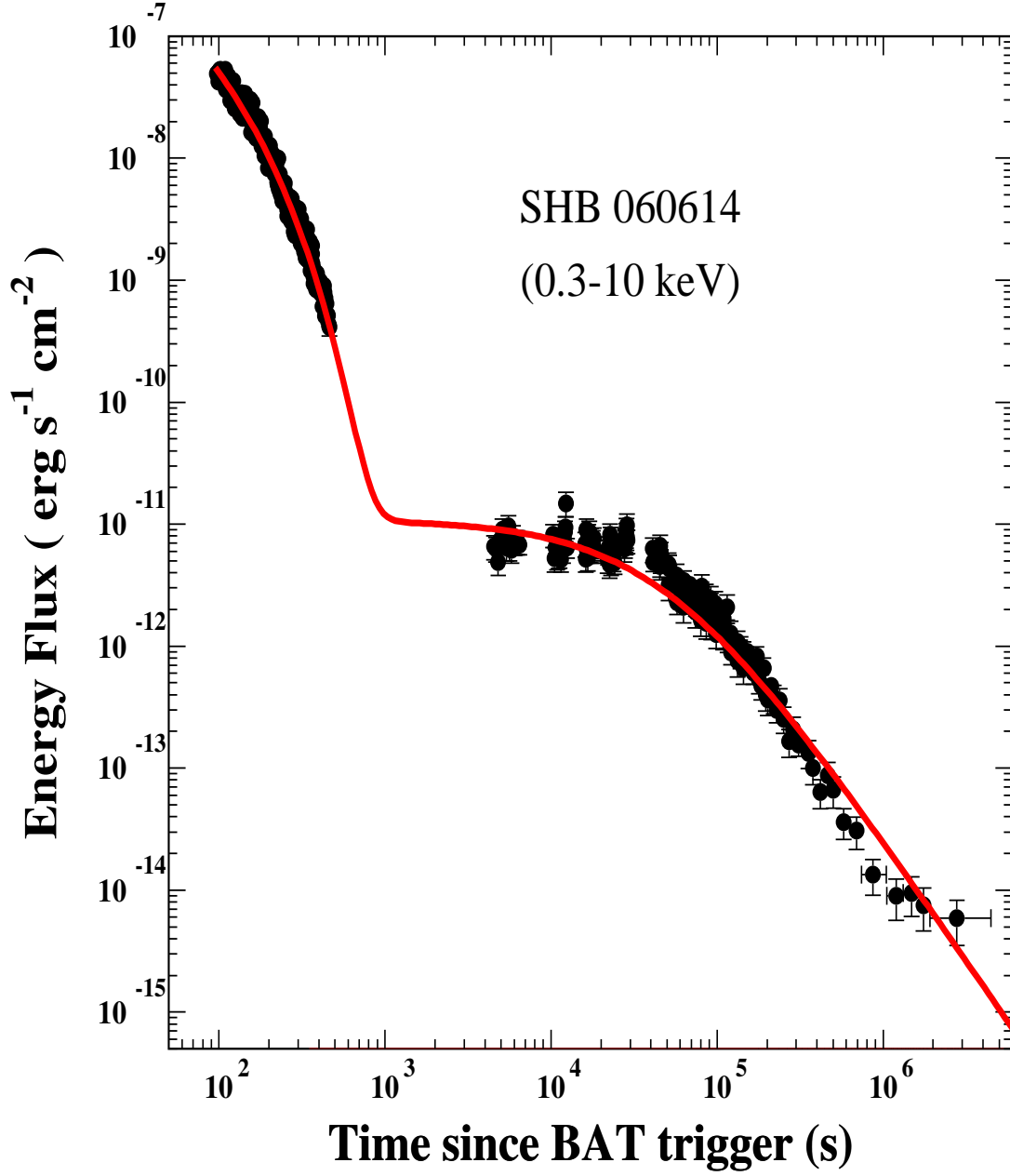


Figure 3. The X-ray light curve of the SN-less GRB 060614 at redshift $z = 0.125$ reported in the Swift-XRT GRB light curve repository (Evans et al. 2007,2009). The line is the best fit light curve as given by Eq.(10) with the parameters listed in Table 2.

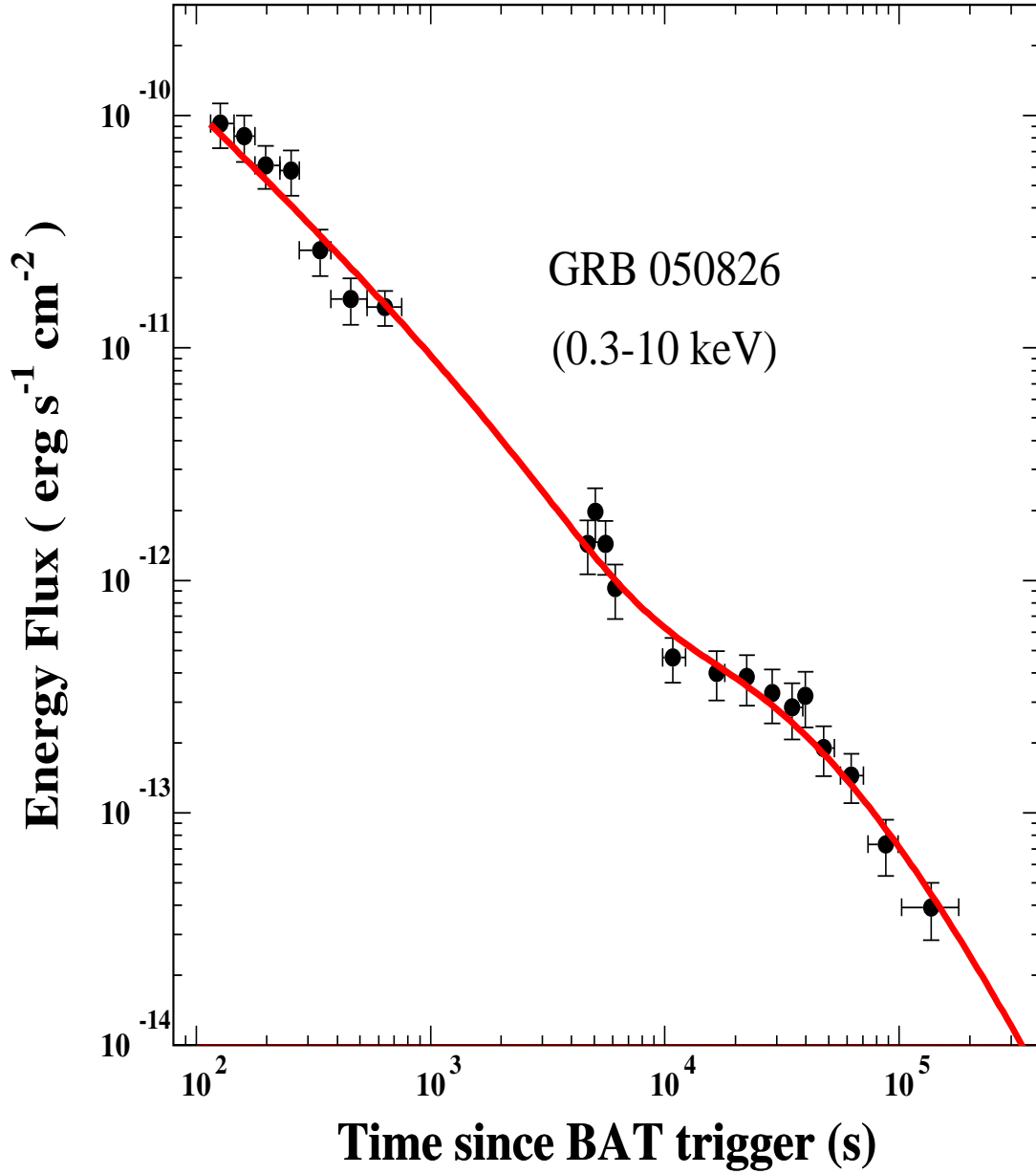


Figure 4. The X-ray light curve of the SN-less GRB050826 at redshift $z = 0.297$ reported in the Swift-XRT GRB light curve repository (Evans et al. 2007,2009). The line is the best fit light curve as given by Eq.(10) with the parameters listed in Table 2.

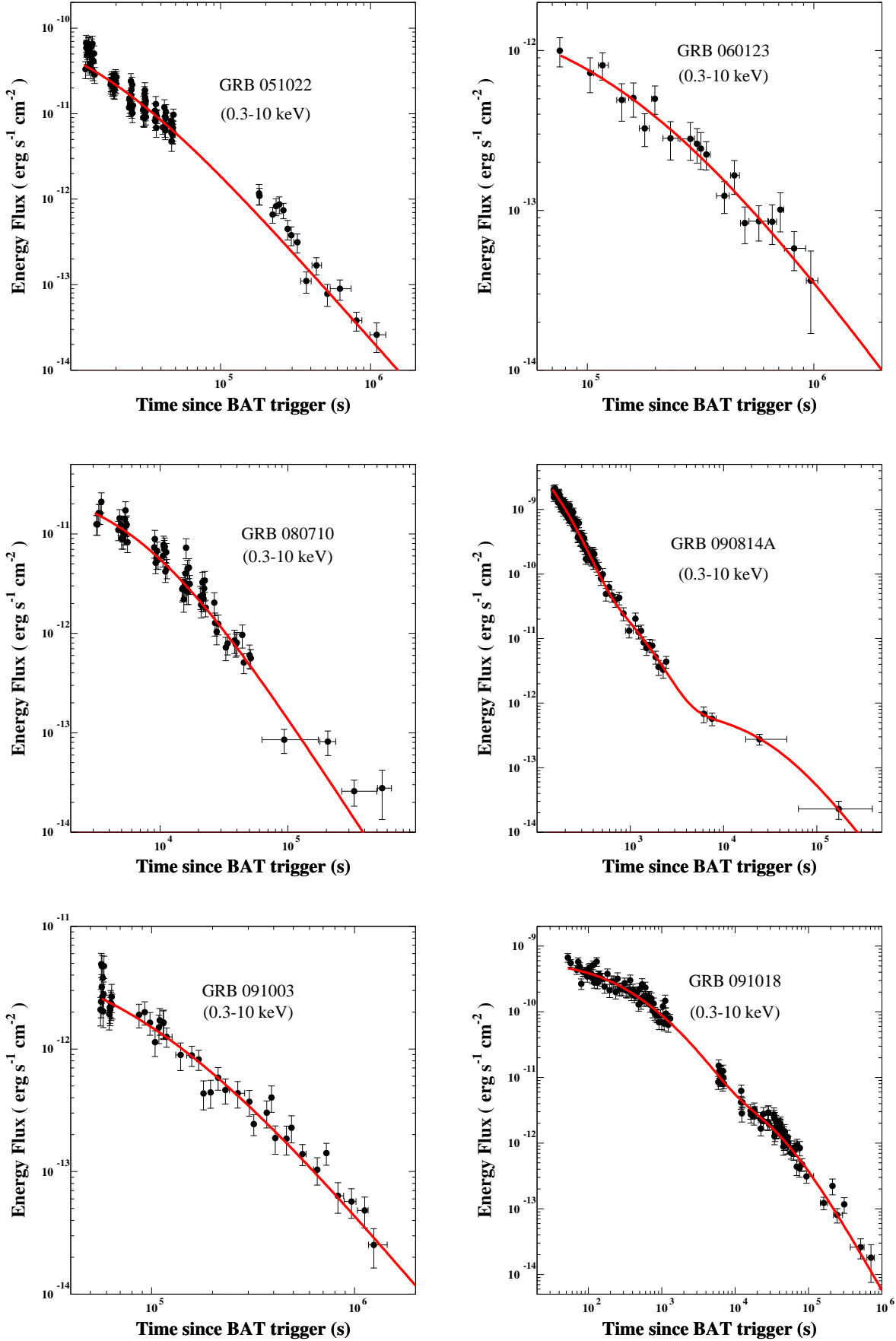


Figure 5. The X-ray light curve of the nearby ($0.15 < z < 1$) SN-less GRBs 051022, 060123, 080710, 090814A, 091003, and 091018 reported in the Swift-XRT GRB light curve repository (Evans et al. 2007,2009) and their best fit light curve for a jet contribution taken over by MSP powered emission, as given by Eq.(10) with the parameters listed in Table 3.

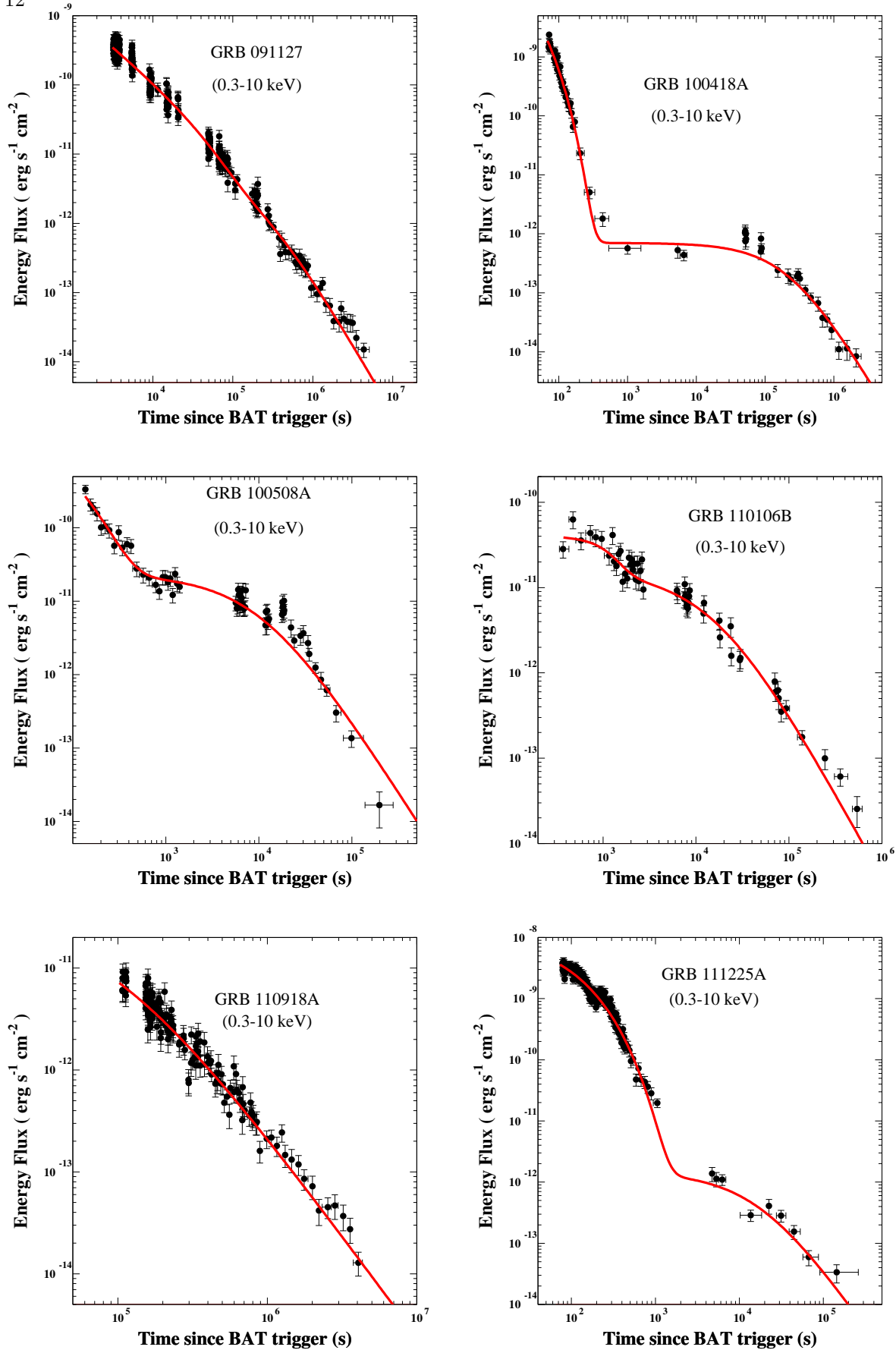


Figure 6. The X-ray light curve of the nearby ($0.15 < z < 1$) SN-less GRBs 091127, 100418A, 100508A, 110106B, 110918A and 111225A reported in the Swift-XRT GRB light curve repository (Evans et al. 2007,2009) and their best fit light curve for a jet contribution taken over by MSP powered emission, as given by Eq.(10) with the parameters listed in Table 3.

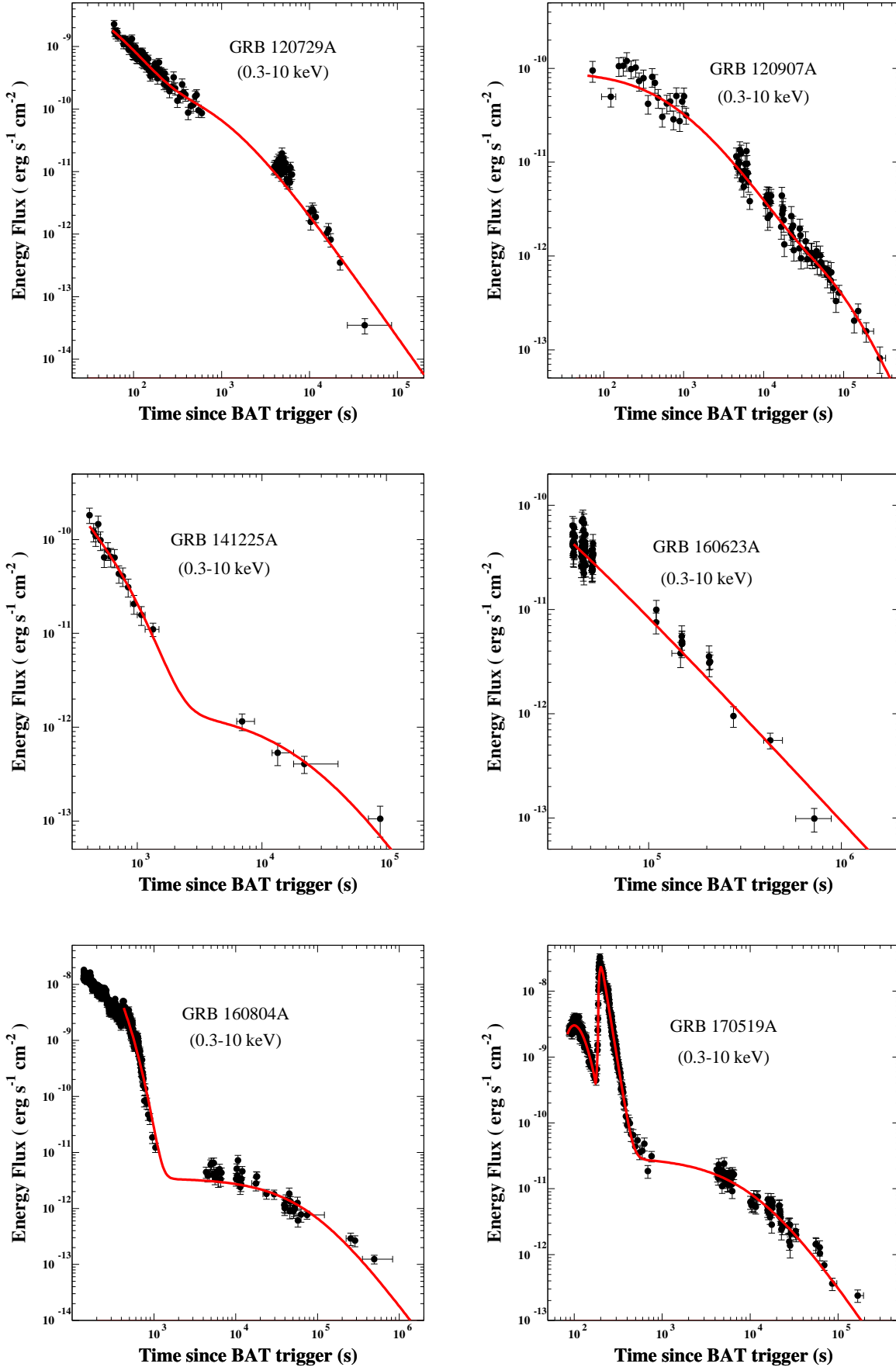


Figure 7. The X-ray light curve of the nearby ($0.15 < z < 1$) SN-less GRBs120729A, 120907A, 141225A, 160623A, 160804A and 170519A reported in the Swift-XRT GRB light curve repository (Evans et al. 2007,2009) and their best fit light curve for a jet contribution taken over by MSP-powered emission, as given by Eq.(10) with the parameters listed in Table 3.

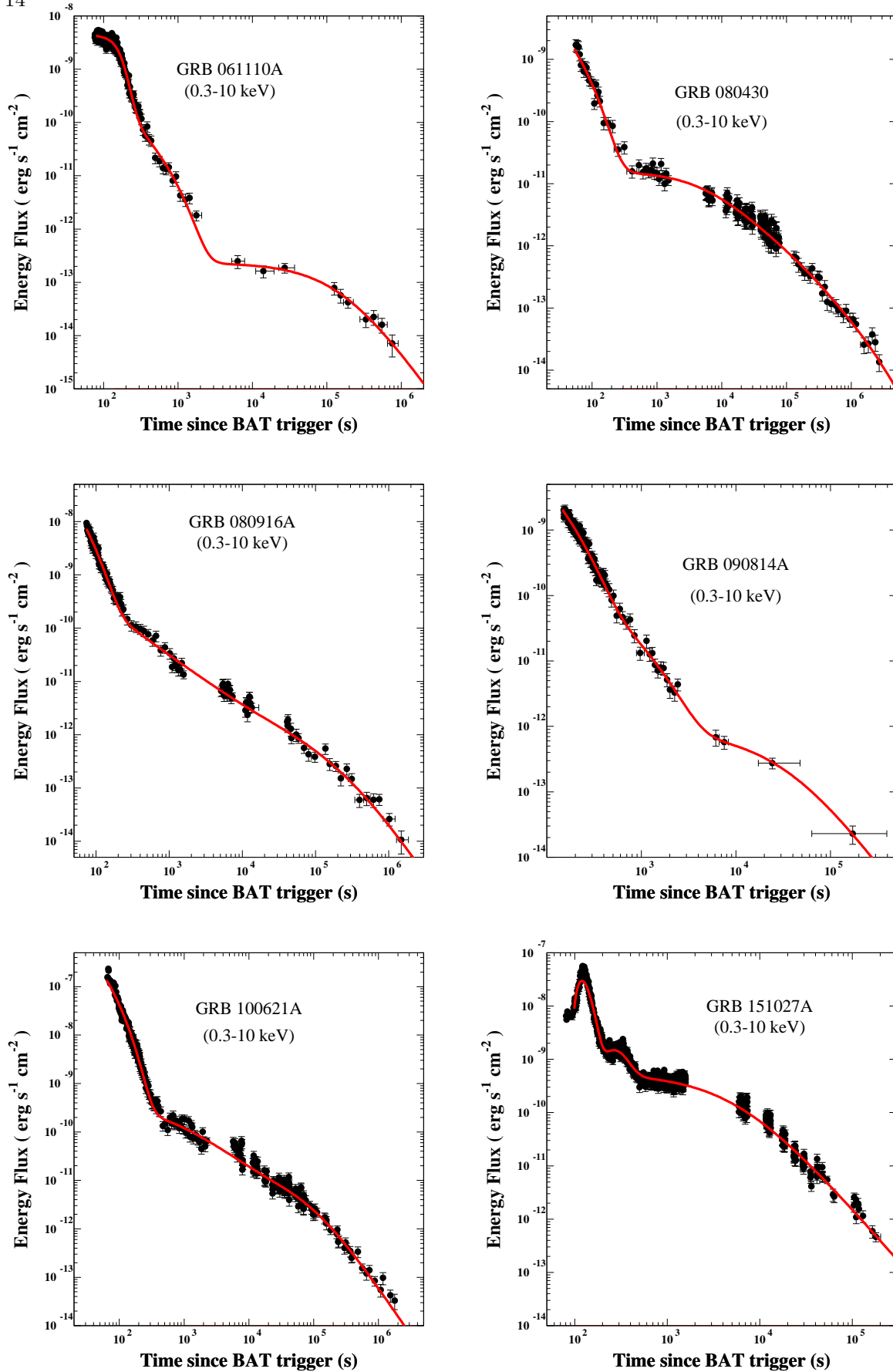


Figure 8. The X-ray light curve of the nearby ($0.15 < z < 1$) SN-less GRBs 061110A, 080430, 080916A, 090814A, 100621A, and 151027A, reported in the Swift-XRT GRB light curve repository (Evans et al. 2007,2009), and their best fit light curve for a jet contribution taken over by MSP powered emission, as given by Eq.(4) plus Eq.(7) with the parameters listed in Table 3.

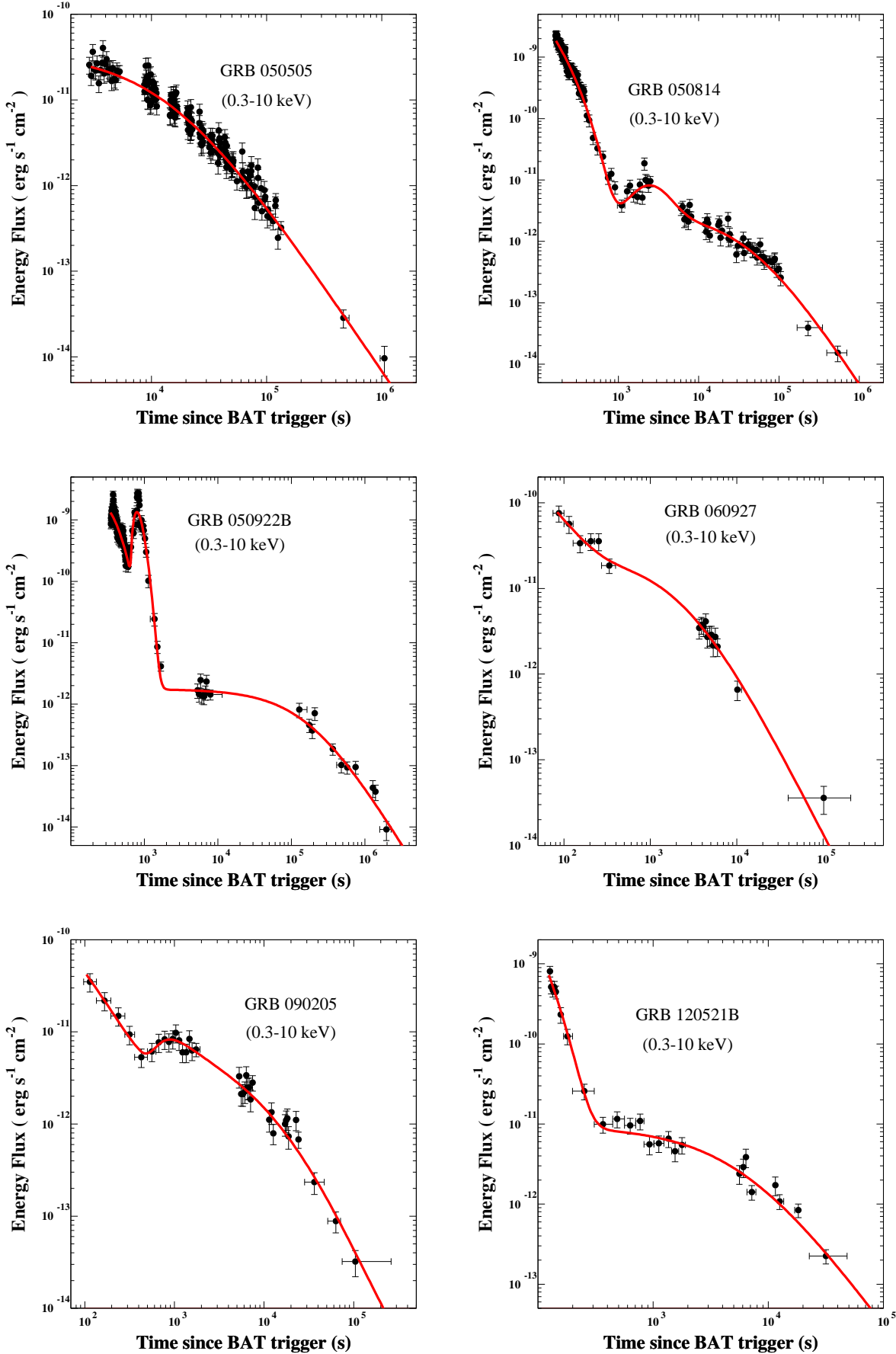


Figure 9. The X-ray light curve of the SN-less GRBs 050505, 050814, 050922B, 060927, 090205, and 120521B with $z > 4$ reported in the Swift-XRT GRB light curve repository (Evans et al. 2007,2009) and their best fit light curve for a jet contribution taken over by MSP powered emission, as given by Eq.(10) or by Eq.(4) plus Eq.(7) with the parameters listed in Table 4.

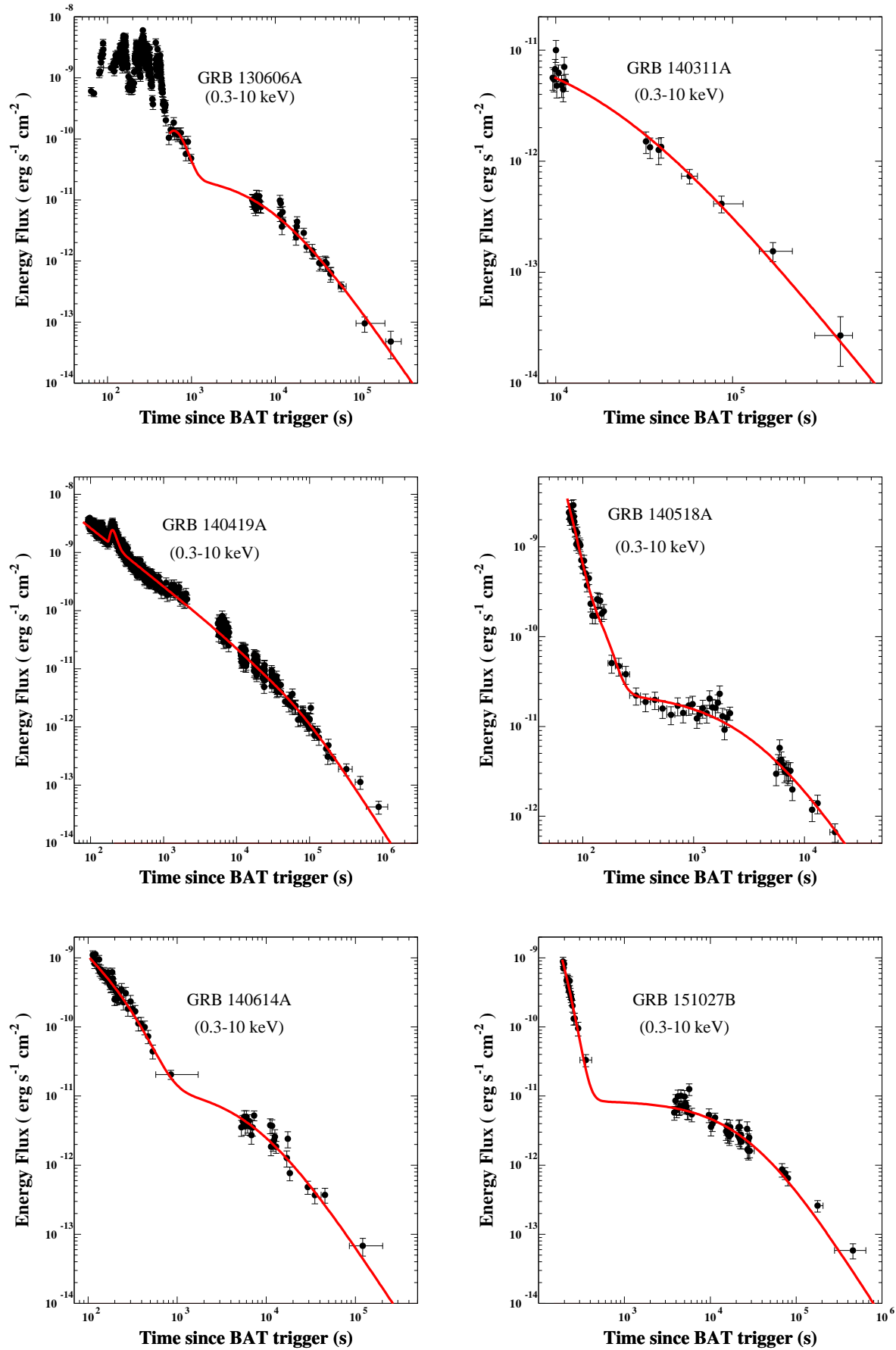


Figure 10. The X-ray light curve of the SN-less GRBs 130606A, 140311A, 140419A, 140518A, 140614A, and 151027B with $z > 4$ reported in the Swift-XRT GRB light curve repository (Evans et al. 2007,2009) and their best fit light curve for a jet contribution taken over by MSP powered emission, as given by Eq.(10) or by Eq.(4) plus Eq.(7) with the parameters listed in Table 4

Table 2. The values of the parameters of Eq.(10) obtained from a best fit to the well-sampled light curves of the X-ray afterglows of the 4 nearest SN-less GRBs ($z < 0.15$) shown in Figures 1-4. Also listed are the values of the periods of the MSPs at birth, as estimated from the best fit valued of F_{ps} and t_b .

SHB	z	F_i [$erg/s\ cm^2$]	a	τ [s]	F_{ps} [$erg/s\ cm^2$]	t_b [s]	χ^2/dof	$P_0/\eta^{1/2}$ [ms]
051109B	0.080 ?	1.79E-7	[0]	15	6.21E-12	5958	2.84	?
080517	0.089	4.83E-8	[0]	153	3.92E-13	33400	2.84	303
060614	0.125	1.64E-7	[0]	111	1.09E-11	49830	1.39	33
050826A	0.297	7.57E-9	[0]	159	2.30E-11	10692	1.10	20

Table 3. The parameters obtained from the best fit light curves to the well-sampled X-ray afterglows of GRBs of known redshift $0.15 < z < 1$, without a confirmed association with SN. The 18 GRBs shown in Figures 5-7 were fit with Eq.(10) and the last 6 GRBs were fit with Eq.(4) plus Eq.(7). Also listed are the periods of the MSPs at birth, as estimated from the best fit values of F_{ps} and t_b . The index i is the pulse number

SHB	z	F_i [$erg/s\ cm^2$]	t_i	τ_i [s]	F_{ps} [$erg/s\ cm^2$]	t_b [s]	χ^2/dof	$P_0/\eta^{1/2}$ [ms]
051022A	0.809		0		1.40E-10	13007	1.48	2.63
060123	0.56		0		2.15E-12	146432	0.85	9.25
080710	0.845		0		3.42E-11	6740	0.85	7.07
090814A	0.696	6.88E-9	0	125	8.46E-13	33274	0.90	71.2
091003	0.8969		0		7.24E-12	83890	1.19	4.10
091018	0.971	5.68E-10	0	4528	7.82E-12	27775	1.14	6.34
091127	0.49	9.61E-9	0	48480	9.38E-12	140532	1.09	5.17
100418A	0.6235	1.76E-8	0	40	7.02E-13	235123	1.56	11.4
100508A	0.5201	1.00E-8	0	163	2.18E-11	12067	2.17	10.9
110106B	0.618	2.55E-11	0	511	1.56E-11	16076	1.42	9.32
110918A	0.982		0		3.61E-11	82033	1.24	1.69
111225A	0.297	9.27E-9	0	237	1.46E-12	17838	1.91	62.2
120729A	0.80	2.08E-8	0	106	3.06E-10	864	2.65	6.98
120907A	0.97	9.07E-11	0	12691	2.38E-12	64579	2.65	7.54
141225A	0.915	3.04E-8	0	542	1.63E-12	23065	0.77	16.2
160623A	0.367		0		2.40E-9	6261	1.15	2.07
160804A	0.736	2.81E-7	0	136	3.47E-12	77312	2.09	7.57
170519A	0.818	3.06E-7	0	52	3.05E-11	11123	1.50	6.05
061110A	0.758	3.97E-9	0	33	2.33E-13	158697	1.26	19.7
		7.76E-11	0	552				
080430	0.768	2.56E-9	0	67	3.64E-13	662118	0.89	7.61
		1.54E-11	0	264243				
080916A	0.689	8.32E-8	0	40	1.22E-12	146113	1.13	9.89
		2.19E-7	0	62767				
090814A	0.696	6.88E-8	0	125	8.46E-13	33274	0.90	40.4
		2.61E-11	0	1332				
100621A	0.542	6.14E-7	0	50	1.53E-11	66116	1.59	5.31
		3.29E-10	0	13750				
151027A	0.81	2.64E-6	91	19	5.37E-10	5563	1.84	2.05
		2.37E-8	173	57				

Table 4. The parameters of the best fit X-ray light curves of well-sampled X-ray afterglow of GRBs of known redshift $z > 4$ which could be well fit by Eq.(10) or by Eq.(4) plus Eq.(7). Also listed are the values of the period of the MSPs at birth, as estimated from the best fit values of F_{ps} and t_b . The index i is the pulse number

SHB	z	F_i [$erg/s\ cm^2$]	t_i	τ_i [s]	F_{ps} [$erg/s\ cm^2$]	t_b [s]	χ^2/dof	$P_0/\eta^{1/2}$ [ms]
050505	4.27				3.56E-11	14058	0.89	1.12
050814	5.77	7.29E-12		140	2.99E-12	41509	1.24	1.79
050922B	4.5				1.76E-12	180862		1.22
060927	5.47	6.05E-11		138	2.45E-11	2403	0.78	3.06
090205	4.65	3.13E-11	0	206	4.46E-12	10622	0.88	3.41
"		4.02E-12	0	34338	$t_{2,0} = 400s$	$\Delta_2 = 382s$		
120521B	6	4.45E-8		41	9.39E-12	6064	1.08	2.56
130606A	5.913				2.68E-11	8512	1.87	1.29
"		2.30E-7		104	$t_{1,0} = 410s$	$\Delta_1 = 5484s$		
140311A	4.954				1.38E-11	17528	1.39	1.44
140419A	3.965	3.25E-11	0	8150	2.89E-11	24340	1.26	1.00
"		7.62E-9	0	22	$t_{2,0} = 172s$	$\delta_2 = 51s$		
140518A	4.707	8.27E-7	0	18	2.47E-11	3804	1.39	2.40
"		1.45E-10	959	21				
140614A	4.233	5.79E-10	0	263	1.42E-11	7168	1.12	2.50
151027B	4.063	1.72E-7	0	48	8.63E-12	27971	0.99	1.68